

Catalyst–Nanostructure Interfacial Lattice Mismatch in Determining the Shape of VLS Grown Nanowires and Nanobelts: A Case of Sn/ZnO

Yong Ding, Pu Xian Gao, and Zhong Lin Wang*

Contribution from the School of Materials Science and Engineering,
Georgia Institute of Technology, Atlanta, Georgia 30332-0245

Received October 31, 2003; E-mail: zhong.wang@mse.gatech.edu

Abstract: Vapor–liquid–solid (VLS) is a well-established process in catalyst-guided growth of nanowires. The catalyst particle is generally believed to be in liquid state during growth, and it is the site for adsorbing incoming molecules; the crystalline structure of the catalyst may not have any influence on the structure of the grown one-dimensional nanostructures. In this paper, using tin particle guided growth of ZnO nanostructures as a model system, we show that the interfacial region of the tin particle with the ZnO nanowire/nanobelt could be ordered (or partially crystalline) during the VLS growth, although the local growth temperature is much higher than the melting point of tin, and the crystallographic lattice structure at the interface is important in defining the structural characteristics of the grown nanowires and nanobelts. The interface prefers to take the least lattice mismatch; thus, the crystalline orientation of the tin particle may determine the growth direction and the side surfaces of the nanowires and nanobelts. This result may have important impact on the understanding of the physical chemical process in the VLS growth.

Introduction

The vapor–liquid–solid (VLS) process¹ has been an important approach in growth of quasi-one-dimensional (1D) nanowires and nanotubes (referred to as 1D nanostructures). In the VLS process, a metal catalyst is rationally chosen from the phase diagram by identifying a metal that is in liquid state at the growth temperature and serves as the site for adsorbing the incoming molecules, but the metal does not form a solid solution with the nanowire; thus, it is phase-separated at the growth front and leads the growth. The metal liquid droplet serves as a preferential site for absorption of gas-phase reactant. Nanowire growth begins after the liquid becomes supersaturated in reactant materials and continues as long as the catalyst alloy remains in a liquid state and the reactant is available.² During the growth, the catalyst droplet directs the nanowire's growth direction and defines the diameter of the nanowire. Ultimately, the growth terminates when the temperature is below the eutectic temperature of the catalyst alloy or the reactant is no longer available. As a result, the nanowires obtained from the VLS process typically have a solid catalyst nanoparticle at the ends with sizes comparable to diameters of the connected nanowires. Metal particles such as Au and Fe are effective for growing nanowires of Si,^{3,4} III-V compound, II-VI compound, and oxide such as Au/ZnO,^{2,5} Fe/SiO₂,⁶ Co/SiO₂,⁷ Ni/Ga₂O₃,⁸ and Ga/SiO₂.⁹

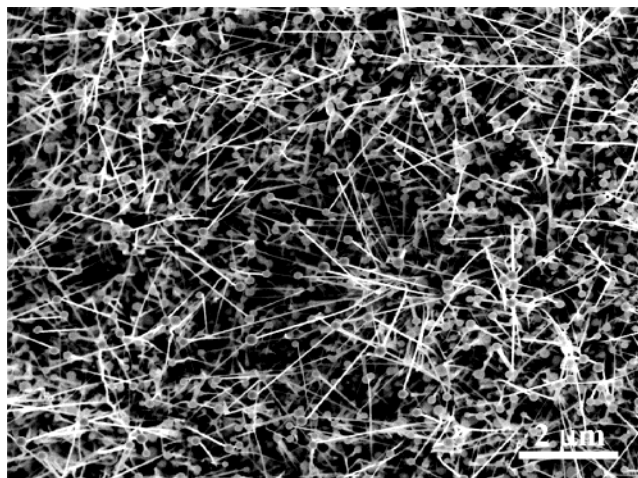


Figure 1. A typical SEM image of the Sn-guided ZnO nanowires and nanobelts.

It is generally believed that the metal particle is a liquid droplet during growth, and its crystal structure in solid may have no influence on the structure of the nanowires and nanobelts to be grown.^{1–9} In this paper, using tin particle guided growth of ZnO 1D nanostructures as a model system, we show

- (1) Wagner, R. S.; Ellis, W. C. *Appl. Phys. Lett.* **1964**, *4*, 89–90.
- (2) Wu, Y. Y.; Yang, P. D. *J. Am. Chem. Soc.* **2001**, *123* (13), 3165–3166.
- (3) Morales, A. M.; Lieber, C. M. *Science* **1998**, *279*, 208–211.
- (4) Cui, Y.; Lathon, L. J.; Gudixsen, M. S.; Wang, J. F.; Lieber, C. M. *Appl. Phys. Lett.* **2001**, *78*, 2214–2216.
- (5) Huang, M. H.; Wu, Y.; Feick, H.; Tran, N.; Weber, E.; Yang, P. *Adv. Mater.* **2001**, *13*, 113–116.

- (6) Liang, C. H.; Zhang, L. D.; Meng, G. W.; Wang, Y. W.; Chu, Z. Q. *J. Non-Cryst. Solids* **2000**, *277*, 63–67.
- (7) Zhu, Y. Q.; Hsu, W. K.; Terrones, M.; Grobert, N.; Terrones, H.; Hare, J. P.; Kroto, H. W.; Walton, D. R. M. *J. Mater. Chem.* **1998**, *8*, 1859–1864.
- (8) Choi, Y. C.; Kim, W. S.; Park, Y. S.; Lee, S. M.; Bae, D. J.; Lee, Y. H.; Park, G. S.; Choi, W. B.; Lee, N. S.; Kim, J. M. *Adv. Mater.* **2000**, *12*, 746–750.
- (9) Pan, Z. W.; Dai, Z. R.; Ma, C.; Wang, Z. L. *J. Am. Chem. Soc.* **2002**, *124* (8), 1817–1822.

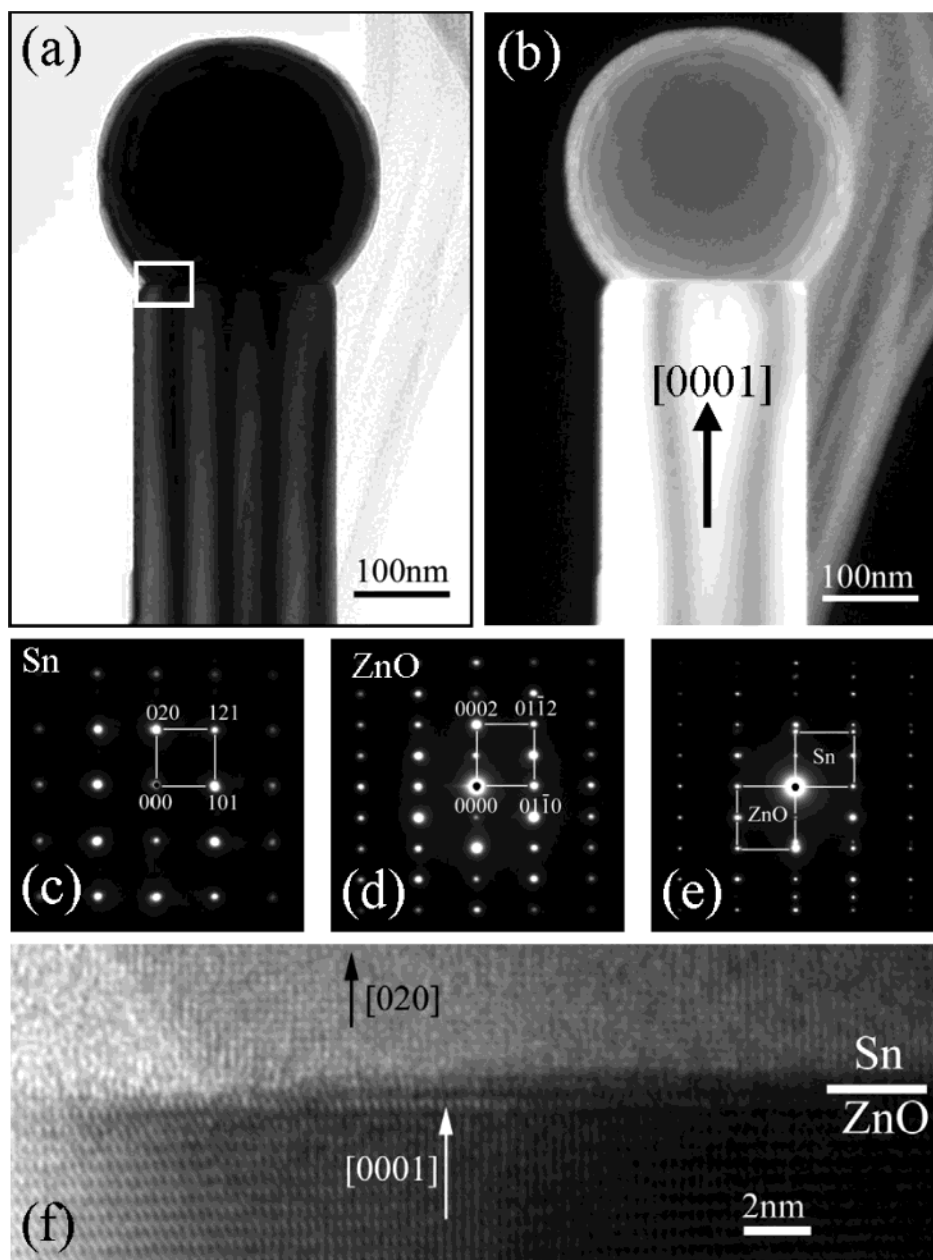


Figure 2. (a) and (b) Bright-field and dark-field images of a [0001] growth ZnO nanowire with an Sn particle at the growth front. (c–e) SAED patterns recorded from the particle, the rod, and both the particle and the rod in (a), respectively. (f) An HRTEM image from the white rectangle-enclosed area in (a) from the interface region.

that the interface between the tin particle and the ZnO nanowire/nanobelt could be partially crystalline or ordered during the VLS growth even though the local growth temperature is much higher than the melting point of the bulk tin, and the crystallographic structure and lattice mismatch at the interface is important in defining the structure characteristics of the grown nanowires and nanobelts. The interface prefers to take the least lattice mismatch; thus, the crystalline orientation of the tin particle may determine the growth direction and the side surfaces of the nanowires and nanobelts. The results may have important impacts for understanding the physical chemical process involved in the VLS growth.

Sample Preparation. The samples used for this study were prepared using a process reported previously.¹⁰ A mixture of

commercial ZnO, SnO₂, and graphite powders in a certain ratio (Zn/Sn/C = 2:1:1) was placed in an alumina boat as the source material and positioned at the center of the alumina tube. The entire length of the tube furnace was 50 cm. The desired nanostructures were deposited onto alumina substrate located in a temperature range of 550–600 °C. The high-resolution transmission electron microscopy (HRTEM) work was carried out using a JEOL-4000EX operated at 400 kV.

Experimental Observation. Figure 1 is a typical scanning electron microscope (SEM) image that shows ZnO nanowires/nanobelts with Sn particles on their tips. Classified from their morphology, the ZnO nanostructures show wire and belt morphologies. Judged from their corresponding selected area electron diffraction (SAED) patterns, we found that ZnO nanowires grow along the [0001] direction and that the nanobelts

(10) Gao, P. X.; Ding, Y.; Wang, Z. L. *Nano Lett.* **2003**, *3*, 1315–1320.

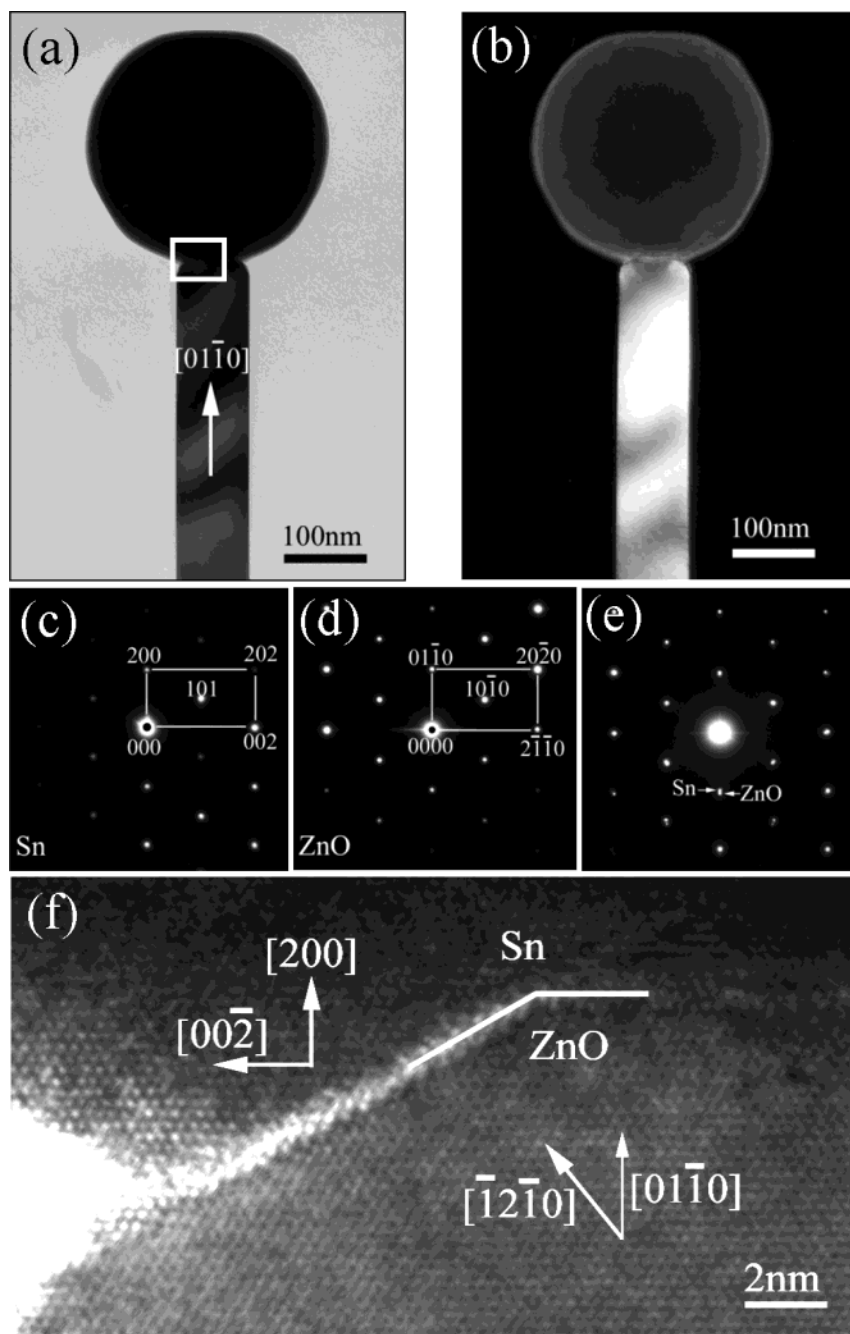


Figure 3. (a) and (b) Bright-field and dark-field images of a $[01\bar{1}0]$ growth ZnO nanobelt with an Sn particle at its tip. (c–e) SAED patterns recorded from the particle, the belt, and both the particle and the belt in (a), respectively. (f) An HRTEM image from the white rectangle-enclosed area in (a).

have two growth directions, $[01\bar{1}0]$ and $[2\bar{1}\bar{1}0]$. No matter which growth direction they take, single crystal Sn particles always exist at their tips, which means that an Sn catalyst can guide not only $[0001]$ growth ZnO nanostructures, but also $[01\bar{1}0]$ and $[2\bar{1}\bar{1}0]$ growth ZnO nanostructures. In the following sections, we will present the orientation relationships in the neck interfaces between Sn particles and the ZnO 1D nanostructures growing along the $[0001]$, $[01\bar{1}0]$, and $[2\bar{1}\bar{1}0]$ directions.

Case 1: $[0001]$ Nanowires. Figure 2, parts a and b, shows bright-field and dark-field images of a nanowire (thickness fringes indicate its wire morphology) with a particle at its tip. The SAED patterns recorded from the particle, the wire, and both the wire and the particle are shown in Figure 2c–e, respectively, and each of them is a single crystal. The SAED

pattern of the particle (Figure 2c) can be indexed as $[10\bar{1}]_{\text{Sn}}$ pattern of the β phase tin with tetragonal structure ($a = 0.5831$ nm, $c = 0.3182$ nm, space group as I_1/amd).¹¹ The SAED pattern of the wire (Figure 2d) belongs to hexagonal ZnO structure with $a = 0.3249$ nm, $c = 0.5206$ nm, space group $P6_3mc$ ¹² and can be indexed to be $[2\bar{1}\bar{1}0]_{\text{ZnO}}$ pattern. The bright-field TEM image combined with SAED pattern reveals that the ZnO nanowire grows along $[0001]$ and that its side surfaces are $\{2\bar{1}\bar{1}0\}$. The interface orientation relationship between the ZnO wire and the Sn particle is $(020)_{\text{Sn}} \parallel (0001)_{\text{ZnO}}$, $[\bar{1}01]_{\text{Sn}} \parallel [2\bar{1}\bar{1}0]_{\text{ZnO}}$. Hereafter,

(11) Joint Committee on Powder Diffraction-International Centre for Diffraction Data (JCPDS-ICDD), 1997, 04-0673.

(12) Gallaso, F. *Structure and Properties of Inorganic Solids*; Pergamon Press: New York, 1970.

we index ZnO using the four-axis notation and the Sn using three-axis notation.

Figure 2f is an HRTEM image of the white rectangle-enclosed area in Figure 2a, which depicts the interface structure between ZnO nanowire and the Sn particle. It is clear that $[0001]_{\text{ZnO}}$ is the growth direction of ZnO nanowire. After measuring the lattice spacing, the $[020]_{\text{Sn}}$ direction of the Sn particle corresponds to ZnO growth direction $[0001]_{\text{ZnO}}$. It is noticed that the interface is flat and the width of the nanowire is comparable to the diameter of the Sn particle. Above the ZnO $(0001)_{\text{ZnO}}$ interface plane, there are two distinction regions, single-crystal Sn particle core and an amorphous shell at the uncovered particle surface, as presented by the dark-field TEM image in Figure 2b. Chemical analysis using energy dispersive X-ray spectroscopy (EDS) indicates that the amorphous layer is SnO_x . It is important to note that the amorphous shell covers only the exposed surface, which may be induced by subsequent oxidation of the Sn particle post growth.

Case 2: $[01\bar{1}0]$ Nanobelts. Figure 3, parts a and b, is bright-field and dark-field TEM images of $[01\bar{1}0]$ growth ZnO nanobelts, respectively. The uniform contrast across its width is distinct from the wire presented in Figure 2a,b. The nanobelts are defined by side surfaces of $(2\bar{1}\bar{1}0)$ and (0001) . The SAED patterns recorded from the Sn particle, the ZnO belt, and both the particle and the belt are shown in Figure 3c–e, respectively. The interface orientation relationship between the particle and the nanobelt is described as $(200)_{\text{Sn}} \parallel (01\bar{1}0)_{\text{ZnO}}$ and $[020]_{\text{Sn}} \parallel [0001]_{\text{ZnO}}$. Figure 3f is an HRTEM image from the white rectangle-enclosed area in Figure 3a from the interface. Compared to the flat interface in the $[0001]$ growth ZnO nanowires, the interface between $[01\bar{1}0]_{\text{ZnO}}$ growth ZnO nanobelt and Sn particle is composed of $(01\bar{1}0)_{\text{ZnO}}$ and $(\bar{1}2\bar{1}0)_{\text{ZnO}}$ planes (corresponding to $(200)_{\text{Sn}}$ and $(30\bar{1})_{\text{Sn}}$, respectively), with a 30° rotation between them. The width of the nanobelts is much smaller than the diameter of the Sn particle.

Case 3: $[2\bar{1}\bar{1}0]$ Nanobelts. Figure 4, parts a and b, is bright-field and dark-field TEM images of a $[2\bar{1}\bar{1}0]$ growth ZnO nanobelt with a Sn particle at its tip. The SAED patterns recorded from the Sn particle, ZnO belt, and both the particle and the belt are shown in Figure 4c–e, respectively. The nanobelt is defined by side surfaces of $(01\bar{1}0)$ and (0001) . The interface orientation relationship can be described as $(002)_{\text{Sn}} \parallel (2\bar{1}\bar{1}0)_{\text{ZnO}}$ and $[020]_{\text{Sn}} \parallel [0001]_{\text{ZnO}}$. Figure 4f is an HRTEM image from the interface. The clear ZnO lattice image in Figure 4f indicates that $[2\bar{1}\bar{1}0]_{\text{ZnO}}$ growth ZnO belt is thin and that the thickness of the belt is uniform. The interface between the particle and belt is flat and composed of $(2\bar{1}\bar{1}0)_{\text{ZnO}}$ and $(200)_{\text{Sn}}$ planes.

As a summary of our data, among the total of 40 nanowires we have studied by TEM, 20 nanowires grow along $[0001]$, 10 grow along $[2\bar{1}\bar{1}0]$, and 10 grow along $[01\bar{1}0]$. The three cases are the only configurations we have identified, and there is no other orientation relationship being found.

Discussion

Catalytic growth of ZnO 1D nanostructures by vapor transport is by a vapor–liquid–solid (VLS) crystal growth process.^{4,5} In our synthesis, the SnO_2 powders were first reduced by carbon into Sn vapor and CO/CO_2 vapor in the high-temperature region, and then the Sn droplet formed on the substrate served as the

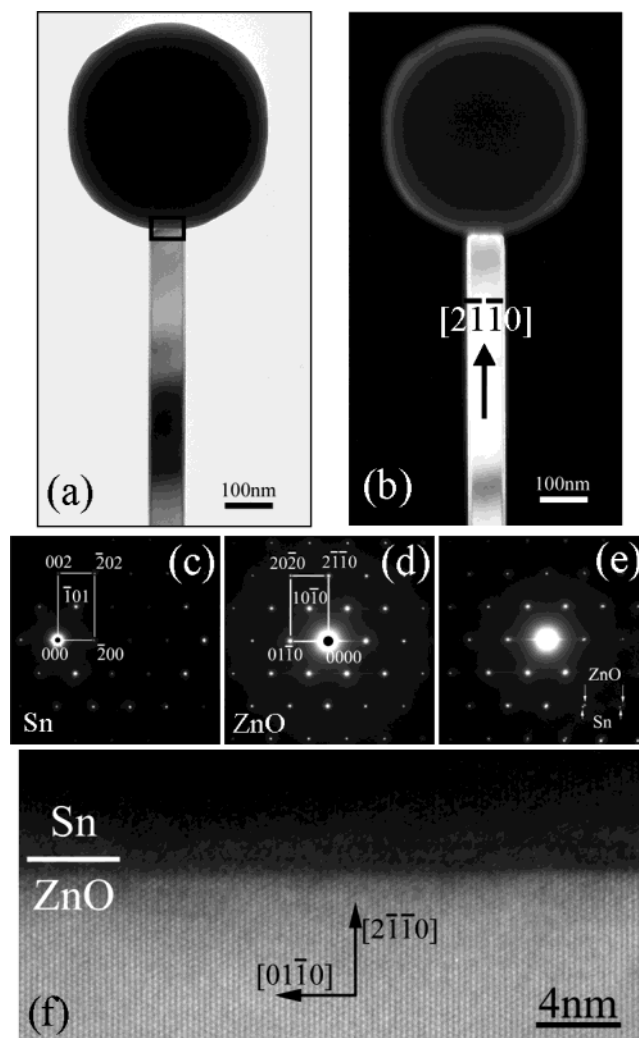


Figure 4. (a) and (b) Bright-field and dark-field images of a $[2\bar{1}\bar{1}0]$ growth ZnO nanobelt with an Sn particle at its tip. (c–e) SAED patterns recorded from the particle, the belt, and both the particle and the belt in (a), respectively. (f) An HRTEM image from the white rectangle-enclosed area in (a).

catalyst. ZnO vapor was transported and adsorbed on the surface of the catalyst. When the alloy droplets became supersaturated, ZnO was phase-separated and crystallized to form the nanowire and nanobelt. Normally, ZnO nanowires prefer to grow along $[0001]_{\text{ZnO}}$ and its diameter is considered to be defined by the catalyst droplets.^{4,5} By choosing a proper substrate, such as $(2\bar{1}\bar{1}0)$ sapphire, ZnO nanowires can grow epitaxially,⁵ which means that the ZnO–substrate interface might control the growth orientation of the ZnO nanostructure. However, no detailed study has been reported on crystal orientation relationship between catalyst and ZnO nanostructures.

When Sn is used as catalyst, some new phenomena appear in our growth that are different from those observed conventionally in nanowire growth: (i) Not only $[0001]$ growth ZnO nanowires, but also considerable amounts of $[01\bar{1}0]$ and $[2\bar{1}\bar{1}0]$ growth ZnO nanobelts have been found, which were grown previously without using catalyst.¹³ (ii) ZnO nanostructures with different growth directions show apparently different sizes although the catalyst Sn particles have about the same size. The ratios between the diameter of the Sn particles and the size of

(13) Pan, Z. W.; Dai, Z. R.; Wang, Z. L. *Science* **2001**, *291*, 1947–1949.

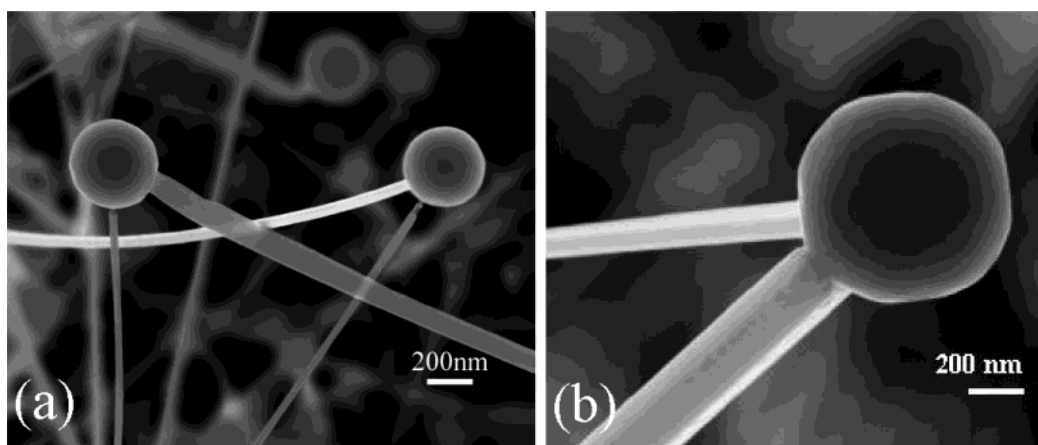


Figure 5. (a) SEM image showing each of the two Sn particles guiding the growth of two ZnO nanobelts. The Sn particle in (b) leads the growth of a ZnO wire and a ZnO belt.

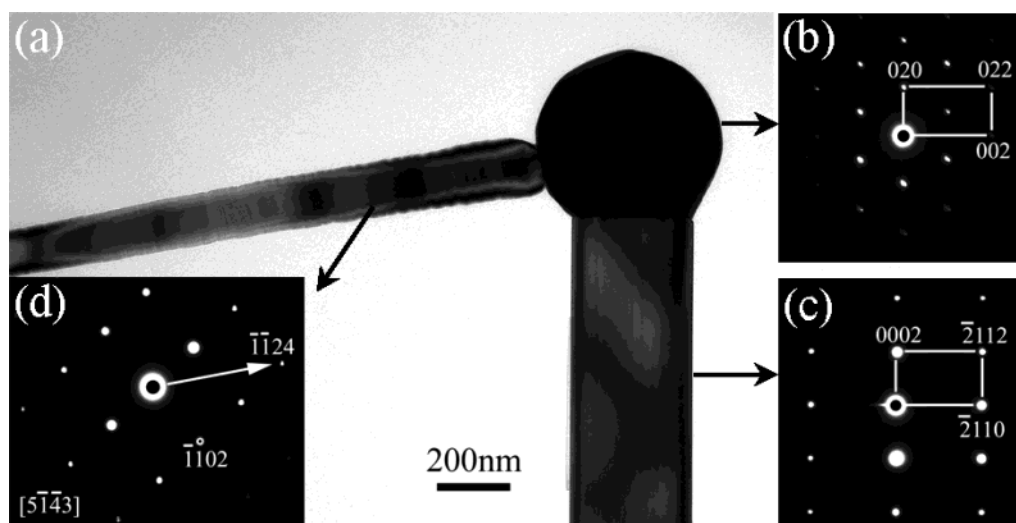


Figure 6. (a) TEM image showing an Sn particle guiding a $[0001]$ growth nanowire and a $[\bar{1}\bar{1}20]$ growth nanobelt at the same time. The SAED pattern of the Sn particle and the $[0001]$ growth nanowire are shown in (b) and (c). (d) SAED pattern recorded from the nanobelt after a small tilting. The incident beam direction is $[5\bar{1}43]$.

the $[0001]$, $[01\bar{1}0]$, and $[2\bar{1}\bar{1}0]$ growing ZnO 1D nanostructures in Figures 2–4 are 1:0.71, 1:0.3, and 1:0.18, respectively. (iii) SAED patterns indicate that ZnO 1D nanostructures in different growth directions have different orientation relationships with the catalyst Sn particle. There are two possibilities for this growth effect: (1) the Sn particle is locally crystallized or atomically ordered at the interfacial region with the ZnO at the initial nucleation and subsequent growth of the 1D nanostructure, so that the crystalline structure of the Sn determines the growth direction and subsequently the side surfaces of the ZnO nanostructure, and (2) the Sn particle was in liquid state during growth, and it crystallized after growth according to the orientation of the 1D nanostructure. The following experimental result gives an unambiguous answer.

An amazing structure observed in the growth product is that one Sn particle results in the growth of two 1D nanostructures along well-defined growth directions. As shown in the SEM images in Figure 5, two 1D ZnO nanostructures can be guided by a single Sn particle. And their morphology indicates that they are in different growth directions. The thin and wide belts from the left Sn particle in Figure 5a grow along $[2\bar{1}\bar{1}0]$ and $[01\bar{1}0]$, respectively; the growth direction of the ZnO wire in

Figure 5b is $[0001]$, while a thin ZnO nanostructure that shares the same Sn catalyst particle shows a belt morphology, with a growth direction of either $[2\bar{1}\bar{1}0]$ or $[01\bar{1}0]$. Figure 6a is a TEM image of two 1D ZnO nanostructures sharing a single Sn catalyst particle. Figure 6b,c is the SAED patterns recorded from the Sn particle and the wide ZnO wire, which indicates that the Sn particle is a single crystal and that the wide ZnO wire grows along $[0001]$. The orientation relationship between the ZnO wire and the Sn particle is the same as the case discussed in Figure 2. After tilting the sample, a zone axis pattern is received from the thin belt (Figure 6d). The projected direction of the nanobelt perpendicular to the beam is $[\bar{1}\bar{1}24]$, indicating that the true growth direction of the belt is $[\bar{1}\bar{1}20]$. The result presented in Figure 6 indicates well-defined crystallographic orientation relationships between the Sn particle and the two 1D nanostructures. Considering the single-crystal structure of the Sn particle after growth, the fixed orientation relationship is only possible if the Sn particle is locally atomically ordered at its surface, although the local growth temperature of ~ 550 – 600 °C is much higher than the bulk melting point of Sn (232 °C).¹⁴

(14) Parish, R. V. *The Metallic Elements*; Longman: New York, 1977.

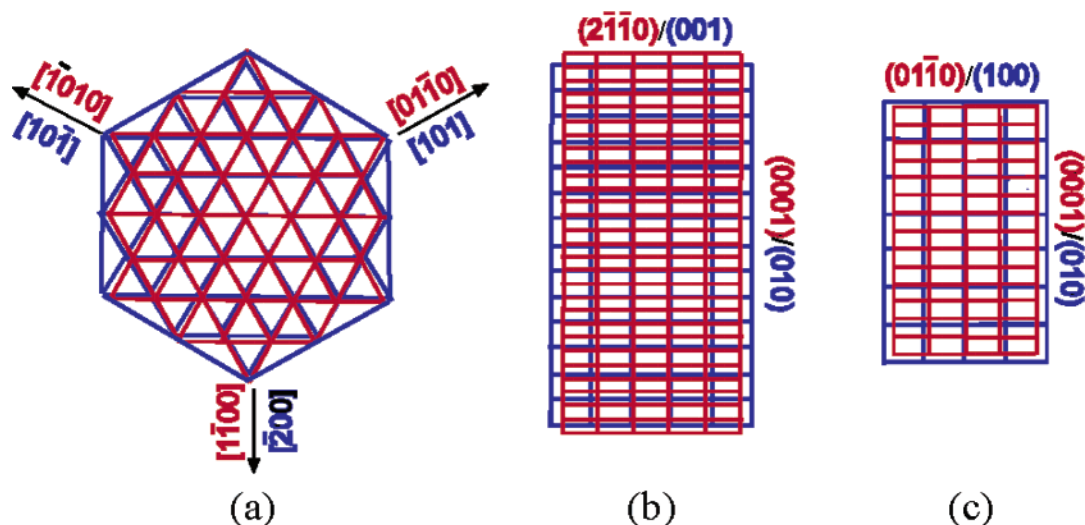


Figure 7. (a–c) Schematics of atomic planes at the epitaxial interfaces between the Sn particle and the $[0001]$, $[01\bar{1}0]$, and $[2\bar{1}\bar{1}0]$ growth ZnO nanostructures, respectively.

This may be possible if there are a few atomic layers of Sn–O on the surface of the Sn particle due to the presence of the oxygen vapor in the growth chamber. Such a local ordering may need to preserve only a few atomic layers in thickness, while the rest of the tin particle is in molten state during growth. Since ZnO has a high melting temperature of 1975 °C,¹⁴ the coherent interfacial “pinning” may raise the local melting temperature of Sn at the interface.¹⁵

The epitaxial orientation relationships between the Sn particle and the ZnO 1D nanostructure can be explained from the *lattice mismatch* at the interface. The schematics in Figure 7 are used to depict the mismatch at the Sn–ZnO interfaces for the three cases presented above. On the basis of the SAED patterns in Figure 2, the interface of $[0001]$ growth nanowire is composed of $(0001)_{\text{ZnO}}$ and $(020)_{\text{Sn}}$ planes. It is known that the atoms in the ZnO $(0001)_{\text{ZnO}}$ plane have 6-fold symmetry. For the $(020)_{\text{Sn}}$ plane matched to $(0001)_{\text{ZnO}}$, the angle between $(101)_{\text{Sn}}$ and $(\bar{1}01)_{\text{Sn}}$ is 57.1°; it is acceptable to consider that the atoms in the $(020)_{\text{Sn}}$ plane have quasi-6-fold symmetry. The low-indexed planes at the interface of ZnO nanostructures are the three sets of $\{01\bar{1}0\}_{\text{ZnO}}$ planes with a 120° angle between them (Figure 7a); two of them match the $\{101\}_{\text{Sn}}$ planes with a lattice mismatch as small as 0.7% in reference to ZnO, and the third one matches the $\{200\}_{\text{Sn}}$ with a lattice mismatch of 3.6%. Thus, hexagon is preferred to be the cross section at the interface, corresponding to a wire/rod morphology.

The interface of $[01\bar{1}0]$ growth ZnO nanobelts is composed of $(01\bar{1}0)_{\text{ZnO}}$ and $(200)_{\text{Sn}}$ planes. The $(0001)_{\text{ZnO}}$ and $(2\bar{1}\bar{1}0)_{\text{ZnO}}$ are the low-indexed perpendicular planes that are matched to $(010)_{\text{Sn}}$ and $(001)_{\text{Sn}}$ planes with lattice mismatches of 12.0 and 2.1%, respectively. The rectangle strain pattern is likely to induce the rectangular belt form. Because the lattice mismatches between $\{2\bar{1}\bar{1}0\}_{\text{ZnO}}$ and $(002)_{\text{Sn}}$ and $\{01\bar{1}0\}_{\text{ZnO}}$ and $(101)_{\text{Sn}}$ are 2.1 and 0.7%, respectively, a possible case is that the lattice mismatch can be reduced by changing the interface from $(01\bar{1}0)_{\text{ZnO}}$ to $(\bar{1}2\bar{1}0)_{\text{ZnO}}$, possibly resulting in the deflection in the interface plane, as observed in Figure 3f.

The asymmetric lattice mismatch also exists in the low-indexed planes of $(0001)_{\text{ZnO}}$ and $(01\bar{1}0)_{\text{ZnO}}$ at the interface of $[2\bar{1}\bar{1}0]$ growing ZnO nanobelts (Figure 7c). The lattice mismatches between $(0001)_{\text{ZnO}}$ and $(020)_{\text{Sn}}$ and $(01\bar{1}0)_{\text{ZnO}}$ and $(200)_{\text{Sn}}$ planes are about 3.6 and 12.0%, respectively. Different from the $[01\bar{1}0]$ growing nanobelts, a larger lattice mismatch of 3.6% exists at the interface between $(01\bar{1}0)_{\text{ZnO}}$ and $(100)_{\text{Sn}}$; thus, the size of the nanobelt is reduced to decrease the interface mismatch energy. The comparably large size of $[0001]$ growth ZnO nanowires is consistent with their small lattice mismatch at the interface.

The orientation relationships between Sn particles and ZnO 1D nanostructures in our synthesis suggest that the Sn particle is partially crystallized or atomically ordered at least at the interface between the particle and the ZnO 1D nanostructure during growth. The ordered layers appear to be taking an important role in initiating the nucleation and growth of the ZnO 1D nanostructure, resulting in morphology control. It may be the reason the 1D ZnO nanostructures from a single Sn particle can take different growth directions, despite the preferred $[0001]$ growth. After the temperature was dropped to room temperature, the Sn particle formed a single-crystal particle, and it preserved the orientation as defined by the interface with the ZnO 1D nanostructure.

Conclusions

Using electron diffraction and high-resolution electron microscopy, we studied the interface relationship between catalyst Sn particles and their guided ZnO 1D nanostructures. Tin catalyst not only can guide $[0001]$ growth nanowires, but it also can guide $[01\bar{1}0]$ and $[2\bar{1}\bar{1}0]$ growth nanobelts. The orientation relationship between the $[0001]$ growth ZnO nanowire and the single crystal β phase Sn particle is $(020)_{\text{Sn}} \parallel (0001)_{\text{ZnO}}$, $[\bar{1}01]_{\text{Sn}} \parallel [2\bar{1}\bar{1}0]_{\text{ZnO}}$. For nanobelts growing along $[01\bar{1}0]$ and $[2\bar{1}\bar{1}0]$, the orientation relationships are $(200)_{\text{Sn}} \parallel (01\bar{1}0)_{\text{ZnO}}$, $[020]_{\text{Sn}} \parallel [0001]_{\text{ZnO}}$ and $(002)_{\text{Sn}} \parallel (2\bar{1}\bar{1}0)_{\text{ZnO}}$, $[020]_{\text{Sn}} \parallel [0001]_{\text{ZnO}}$, respectively. One tin particle can initiate the growth of two 1D nanostructures; the tin particle is single crystal after growth, and it preserves epitaxial relationships with the grown nanostructures.

(15) Zhang, L.; Jin, Z. H.; Zhang, L. H.; Sui, M. L.; Lu, K. *Phys. Rev. Lett.* **2000**, *85*, 1484.

Our results provide new insights in revealing the process involved in VLS growth. Using Sn/ZnO as a model system, we showed that the interfacial region of the tin particle with the ZnO nanowire/nanobelt could be partially crystalline or atomically ordered during the VLS growth, although the local growth temperature is much higher than the melting point of tin, and it may play a key role in initiating 1D nanostructure. The interface prefers to take the least lattice mismatch, thus,

the crystalline orientation of the tin particle may determine the growth direction and the side surfaces of the nanowires and nanobelts.

Acknowledgment. This work was supported by NSF (DMR-9733160) and NASA Vehicle Systems Program and Department of Defense Research and Engineering (DDR&E).

JA039354R